

Ground State Phase Diagram of 2D Electrons in High Magnetic Field

Naokazu SHIBATA and Daijiro YOSHIOKA

Department of Basic Science, University of Tokyo, Komaba 3-8-1 Meguro-ku, Tokyo 153-8902, Japan

(Received October 23, 2002)

The ground state of 2D electrons in high magnetic field is studied by the density matrix renormalization group method. The ground state energy, excitation gap, and pair correlation functions are systematically calculated at various fillings in the lowest and the second lowest Landau levels. The ground state phase diagram, which consists of incompressible liquid state, compressible liquid state, stripe state, pairing state, and Wigner crystal is determined.

KEYWORDS: fractional quantum Hall effect, stripe, pairing, Wigner crystal, ground state, phase diagram, two dimension, density matrix, renormalization group

§1. Introduction

Electrons in high magnetic field in two dimensional systems exhibit various interesting phenomena as a typical many body interacting system. In two dimensional systems, kinetic energy of electrons is completely quenched by perpendicular magnetic field and remaining macroscopic degeneracy is lifted by Coulomb interaction. This is the origin of many exotic behaviors of quantum Hall systems and the reason why much effort has been needed to understand these systems.

As typical ground states in strong magnetic field, Laughlin state and Wigner crystal have attracted much attention. Laughlin state is a quantum liquid with an excitation gap, which is an exact ground state for strong short range repulsive interaction at $\nu = 1/(2m + 1)$.¹⁾ On the other hand, Wigner crystal is the ground state of classical point particles realized in the limit of strong magnetic field. Their relative stability depends on the ratio between the magnetic length $\ell = (\hbar c/eB)^{1/2}$, which is the length scale of one particle wave function, and the mean distance between the electrons $\sim n^{-1/2}$ given by the density n of two-dimensional electrons. Thus the determination of the ground state phase diagram with respect to the filling factor $\nu = 2\pi\ell^2 n$ is an interesting issue for understanding the competition between completely different electronic states.

Experimentally, clear fractional quantum Hall effect has been observed at $\nu = 1/3$,²⁾ which is naturally explained by Laughlin state,¹⁾ and exact numerical diagonalizations confirmed its existence in the lowest Landau level.³⁾ The formation of Wigner crystal has been supported by experiments on transport properties at low fillings $\nu \lesssim 1/5$, where observed insulating behavior is explained by the pinning of Wigner crystal by residual potential fluctuations.^{4,5)}

With decreasing magnetic field, part of electrons occupy higher Landau levels. In higher Landau levels, one particle wave function extends over space with oscillations, and this change modifies effective interaction between the electrons in each Landau level. Since ex-

tended one particle wave function generates long range exchange interaction, Laughlin state stabilized by strong short range interaction will be unstable. Instead, long range interaction favors charge density waves (CDW's). Within a Hartree-Fock approximation, Koulakov *et al.* showed that CDW's called 'stripe' and 'bubble' are stable against Laughlin state in higher Landau levels with index $N \geq 2$.^{6,7)} After their calculations, anisotropic resistivity consistent with uniaxial electronic state of stripe order has been experimentally observed.^{8,9,10)}

In the second lowest Landau level, more interesting ground states are expected. At $\nu_N = 1/2$, where ν_N is the filling factor of partially filled Landau level, BCS type pairing state has been proposed^{11,12,13)} to explain even denominator fractional quantum Hall effect.¹⁴⁾ Around $\nu_N = 0.4$ and $\nu_N = 0.24$, reentrant integer quantum Hall effects have been observed.¹⁵⁾ At $\nu_N = 1/3$ and $1/5$, fractional quantum Hall effects have been observed.^{14,15)} The origin of these phenomena is still unclear and systematic study is needed.

In order to identify diverse ground states and determine the ground state phase diagram, we have to solve quantum many body problem of Coulomb interaction. In the present study we use the density matrix renormalization group (DMRG) algorithm^{16,17)} to deal with large size systems extending limitation of exact diagonalizations, and systematically calculate the ground state wave function and excitation energies for the lowest and the second lowest Landau levels. Based on the pair correlation functions and the excitation energies, we determine the ground state phase diagram, which consists of incompressible liquid state, compressible liquid state, stripe state, pairing state, and Wigner crystal.

§2. Model and Method

The Hamiltonian for electrons in Landau levels contains only Coulomb interaction. After the projection onto the Landau level with index N , the Coulomb in-

teraction is written as

$$H = \sum_{i < j} \sum_{\mathbf{q}} e^{-q^2/2} [L_N(q^2/2)]^2 V(q) e^{i\mathbf{q} \cdot (\mathbf{R}_i - \mathbf{R}_j)}, \quad (2.1)$$

where \mathbf{R}_i is the guiding center coordinate of the i th electron, which satisfies the commutation relation, $[R_j^x, R_k^y] = i\ell^2 \delta_{jk}$, $L_N(x)$ are the Laguerre polynomials, and $V(q) = 2\pi e^2/\varepsilon q$ is the Fourier transform of the Coulomb interaction. The magnetic length ℓ is set to be 1, and we take $e^2/\varepsilon\ell$ as units of energy scale. We omit the component at $q = 0$, which is canceled by uniform positive background charge. We assume completely spin polarized ground state and neglect the electrons in fully occupied Landau levels. We also assume that the width of the wave function perpendicular to the two dimensional plane is sufficiently small compared with ℓ .

In order to obtain the ground state of the Hamiltonian, we employ the DMRG method.^{16,17)} This method enables us to calculate ground state wave function of large systems with controlled accuracy. The algorithm of this method is summarized as follows: We start from a small system, i.e. a system consisting of only four local orbitals. We divide the system into two blocks, and add new orbitals at the end of two blocks to expand the blocks. We then calculate the ground state wave function of the total system and obtain the density matrix of each expanded blocks. We then restrict the basis states in the expanded blocks by keeping only eigenstates of large eigenvalues of the density matrix. We add new orbitals again and repeat the above procedure until we get desired size of system. We then use the finite system algorithm of the DMRG to improve the ground state wave function. After several sweeps, we obtain the most optimal ground state within the restricted number of basis states. The error due to the truncation of basis states is estimated from the eigenvalues of the density matrix, and the accuracy of the wave function is systematically improved by increasing the number of basis states kept in the blocks.

§3. Results

In the following, we calculate ground state wave function of the Hamiltonian for Landau levels of $N = 0$ and 1. We study various size of systems with up to 25 electrons in the unit cell of $L_x \times L_y$ with periodic boundary conditions in both x and y directions. We choose the aspect ratio L_x/L_y by the position of the energy minimum with respect to L_x/L_y in order to avoid artificial determination of the periodicity of CDW's. The truncation error in the DMRG calculation is typically 10^{-4} for 25 electrons with 180 states in each blocks. The existing results of exact diagonalizations are completely reproduced within the truncation error. Since the present Hamiltonian has the particle-hole symmetry, we only consider the case of $\nu_N \leq 1/2$.

3.1 Compressible liquid at $\nu = 1/2$

We first investigate the ground state at $\nu = 1/2$ in the lowest Landau level. Since the denominator of ν is even and the filling factor is large, the ground state is neither

Laughlin state nor Wigner crystal. Based on the composite fermion theory, the flux attached to the electrons completely cancels external magnetic field within the mean field level and Fermi liquid ground state is expected.^{18,19)} Indeed, experiments show saturation in longitudinal resistivity at low temperatures,²⁰⁾ which is consistent with Fermi liquid like compressible ground state.

In order to confirm the compressible ground state, we first analyze size dependence of the excitation gap. The obtained results for systems with up to 25 electrons are shown in Fig. 1. Although the excitation gap does not follow single scaling function, all the results are smaller than the upper bound shown by the dashed line, which is proportional to $N_s^{-1/2}$, where N_s is the number of one-particle states in the unit cell. We thus expect vanishing of the excitation gap in the thermodynamic limit. We find small excitation gap at small number of electrons. Such vanishing excitation gap appears for free electrons in the square unit cell at $N_e = 2, 3, 4, 6, 7, 8, 10, 11, 12, 14, 15, \dots$, with periodic boundary conditions. This means large excitation gap appears only at $N_e = 1, 5, 9, 13, 21, 25, \dots$, where electrons occupy all the degenerate states forming closed shell. The present result of interacting system also shows a shell structure but it is not the same to that of free electrons in contrast to the results in the spherical geometry, where the same shell structure is obtained.²¹⁾ Nevertheless, the estimated effective mass $1/m^*$ of the composite fermion determined from the value of the gap at $N_e = 9$ and 25 is 0.12 and 0.27, respectively, in units of $e^2/\varepsilon\ell$, which are roughly consistent with the result 0.20 obtained from the exact diagonalizations in the system of spherical geometry.²¹⁾

In Fig. 2 (a) we show the ground state pair correlation function defined in the following equation:

$$g(\mathbf{r}) \equiv \frac{L_x L_y}{N_e(N_e - 1)} \langle \Psi | \sum_{i \neq j} \delta(\mathbf{r} + \mathbf{R}_i - \mathbf{R}_j) | \Psi \rangle, \quad (3.1)$$

where $|\Psi\rangle$ is the ground state. The correlation function is circularly symmetric and short range power law exponent is two as shown in Fig. 3. These results are also consistent with gapless liquid ground state.

3.2 Incompressible liquids at $\nu = n/(1 + 2n)$

When we decrease filling factor from $1/2$, fractional quantum Hall effects are experimentally observed at various fractional fillings.^{22,23)} In particular, the primary series of $\nu = n/(1 + 2n)$ with $n = 1, 2, 3, 4, 5$ is well known for its large excitation gap. Here, we confirm the existence of excitation gap at $\nu = n/(1 + 2n)$ by systematically calculating the lowest excitation gap for filling factors between $\nu = 0.3$ and 0.5. The obtained result for systems with 12, 14, 15, 16, 18, 20, 24, and 25 electrons are shown in Fig. 4. As is clearly seen, large excitation gap is obtained for $\nu = n/(1 + 2n)$. The size of the gap decreases with increasing n , and its dependence is consistent with experiments. Based on the composite fermion theory, the effective mass is estimated from the excitation gap. The estimated value of $1/m^*$ in units

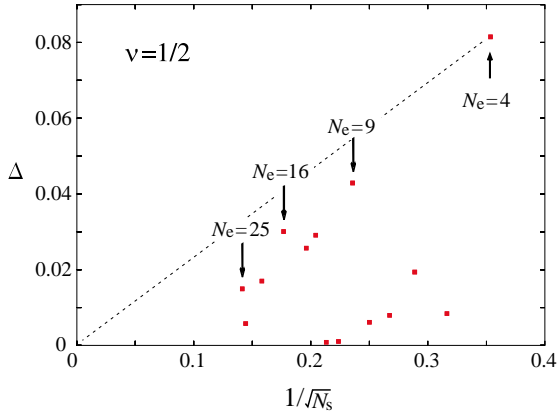


Fig. 1. Size dependence of the lowest excitation gap at $\nu = 1/2$ for various number of electrons N_e in square unit cell. N_s is the number of one-particle states in the unit cell. The dashed line is a guide for eyes.

of $e^2/\varepsilon\ell$ is around 0.23, which is almost the same to the value ~ 0.2 determined at $\nu = 1/2$. We mention that the composite fermion picture also predicts small excitation gap in finite system at $\nu = 4/11$,²⁴⁾ which is consistent with the present result shown in Fig. 4.

In order to confirm liquid ground state at $\nu = n/(1 + 2n)$, we next see the ground state pair correlation functions. The results for $\nu = 5/11$, $2/5$, and $1/3$ are shown in Figs. 2 (b), (c) and (f), respectively. As is seen, the correlation functions are circularly symmetric, which confirms liquid ground state.

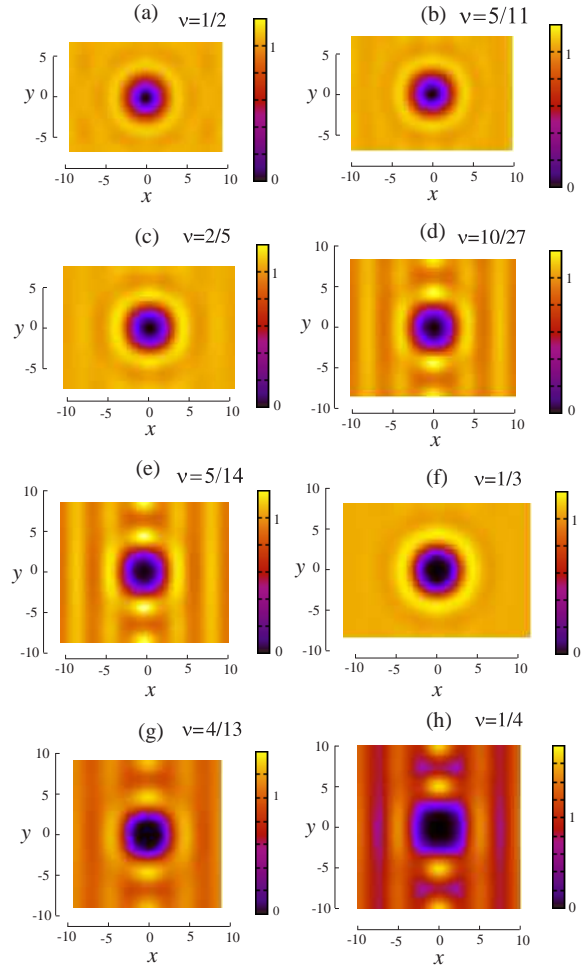


Fig. 2. Ground state pair correlation functions in the lowest Landau level for various ν . $N_e = 20$ for $\nu = 1/2$, $5/11$, $2/5$, $10/27$, $5/14$, and $1/3$. $N_e = 16$ for $\nu = 4/13$ and $1/4$.

3.3 Weak stripes below $\nu \sim 0.42$

We next consider almost gapless ground state between the incompressible liquid states. In Figs. 2 (d), (e), (g), and (h), the pair correlation functions at $\nu = 10/27$, $5/14$, $4/13$ and $1/4$ are shown. We find weak stripe correlations. Similar stripes are observed for $\nu \lesssim 10/24$ except around the incompressible states at $\nu = 2/5$ and $1/3$. The stripe correlations are gradually enhanced with decreasing ν as shown in Fig. 5. We think the gradual enhancement in the stripe correlations are due to the instability to Wigner crystal, and quantum fluctuations partially melt Wigner crystal to form stripe ground state. In fact, short range correlations below $r \sim 5\ell$ are almost the same to that of Wigner crystal. This is clearly different from the stripe state observed in higher Landau levels, where anisotropic resistivity is experimentally observed. The difference from the stripe state in higher Landau levels is clearly shown in §3.4. We note that the present results are different from those obtained in recent studies around $\nu = 3/8$, where stripe state with much longer period of 10ℓ ²⁵⁾ and bubble state around $\nu = 3/8$ ²⁶⁾ are predicted based on the composite fermion theory. The present DMRG results show that the period

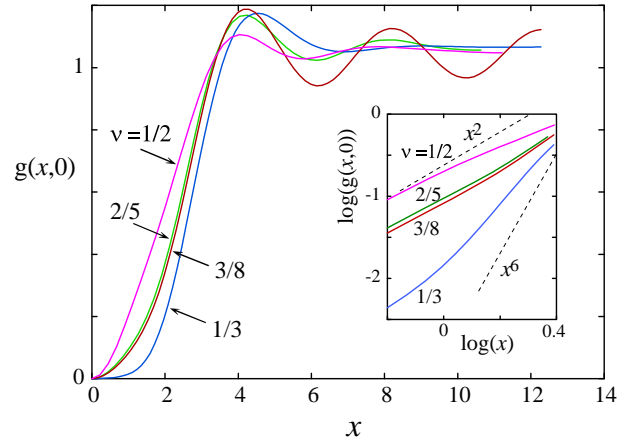


Fig. 3. Pair correlation functions in the lowest Landau level for various ν near half filling. Inset shows logarithmic plot near the origin.

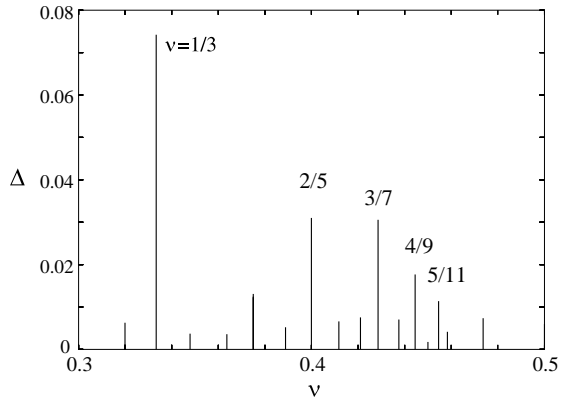


Fig. 4. The lowest excitation gap at various ν . The number of electrons N_e is between 12 and 25.

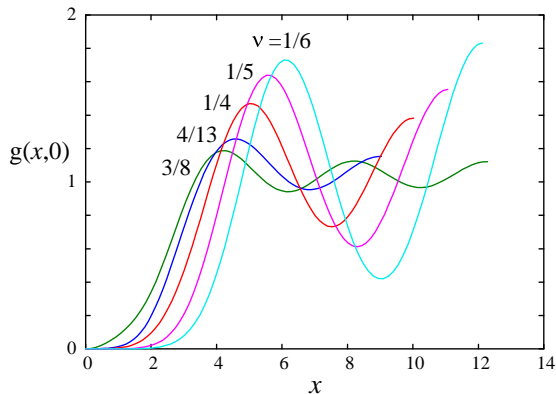


Fig. 5. Ground state pair correlation functions in the lowest Landau level at various ν . $N_e = 24$ for $\nu = 3/8$. $N_e = 16$ for $\nu = 4/13$ and $1/4$. $N_e = 12$ for $\nu = 1/5$ and $1/6$.

of the stripes at $\nu = 3/8$ is about 4ℓ as shown in Fig. 3 and the stripe state is stable in wide range below $\nu \sim 0.42$ except around incompressible state at $\nu = 2/5$ and $1/3$. Detailed study at $\nu = 3/8$ with small size dependence of the stripes will be published elsewhere.

3.4 Laughlin state and stripe order at $\nu = 1/5$

The stripe correlation in the ground state is enhanced with decreasing ν . The correlation function is anisotropic even at $\nu = 1/5$ as shown in Fig. 6 (b), and it is not clear whether there exist transition to incompressible state around $\nu \sim 1/5$. In order to identify the ground state at $\nu = 1/5$, we introduce Haldane's pseudo potentials V_m between the electrons.²⁷⁾ It is shown that the Laughlin state at $\nu = 1/5$ is an exact ground state for strong short range repulsive interaction consisting of only V_1 and V_3 , which act only between electron pairs whose relative angular momentum m is 1 and 3, respectively. Thus we can see how the ground state connects to Laughlin state with increasing V_1 and V_3 from its values of the pure Coulomb interaction. If there exist no phase transition, the ground state is in the same phase characterized by

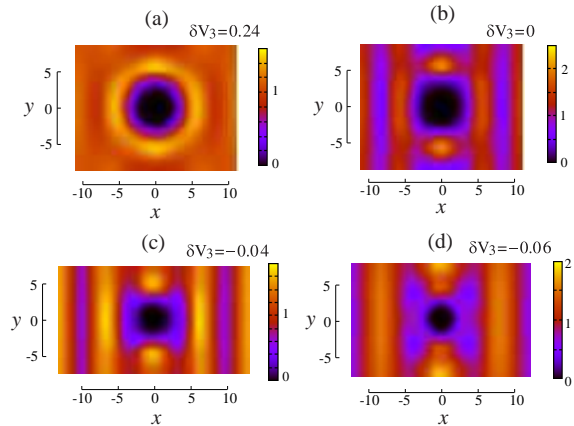


Fig. 6. Ground state pair correlation functions at $\nu = 1/5$ for various δV_3 . $N_e = 12$. $\delta V_3 = 0$ corresponds to pure Coulomb interaction.

Laughlin state.

In order to clarify whether there is a phase transition, we calculate the low energy excitations as a function of V_3 . Since V_1 of pure Coulomb interaction is already large in the lowest Landau level with a small probability of finding electron pairs whose relative angular momentum is 1 for $\nu < 1/3$, we change only V_3 .

Figure 7 shows the V_3 -dependence of the ground state energy and the first excited state energy at $\nu = 1/5$ with 12 electrons. With increasing V_3 from $\delta V_3 = 0$, the ground state energy monotonically changes and the excitation gap continuously increases. The ground state correlation function at $\delta V_3 = 0.24$ shown in Fig. 6 (a) is circularly symmetric and it is well characterized by Laughlin state. Since no phase transition is detected, the ground state of pure Coulomb interaction belongs to the same phase of Laughlin state.

When we decrease V_3 from $\delta V_3 = 0$, however, significant change occurs in the ground state. As shown in Fig. 7, the slope of the ground state energy clearly changes at $\delta V_3 = -0.04$. This change in the ground state energy reflects the qualitative change in short range correlation functions. As is shown in Fig. 8, the shoulder structure at $x \sim 3\ell$ develops below $\delta V_3 \sim -0.04$ and it makes clear anisotropy around $r \sim 4\ell$. The shape of the correlation function for $\delta V_3 < -0.04$ is almost the same to that realized in higher Landau levels and clearly different from the stripe structure of pure Coulomb interaction in the lowest Landau level around $\nu = 1/5$.

3.5 Transition to Wigner crystal

In the limit of low filling, the magnetic length ℓ becomes negligible compared with the mean distance between the electrons. Since ℓ is the length scale of one particle wave function, the electrons can be treated as classical point charges, and the ground state is expected to be Wigner crystal. In order to confirm the existence

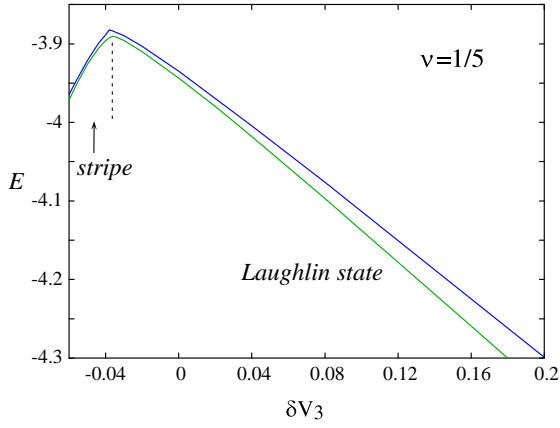


Fig. 7. V_3 dependence of the ground state and first excited state energies at $\nu = 1/5$ in the lowest Landau level. $N_e = 12$. $\delta V_3 = 0$ corresponds to pure Coulomb interaction.

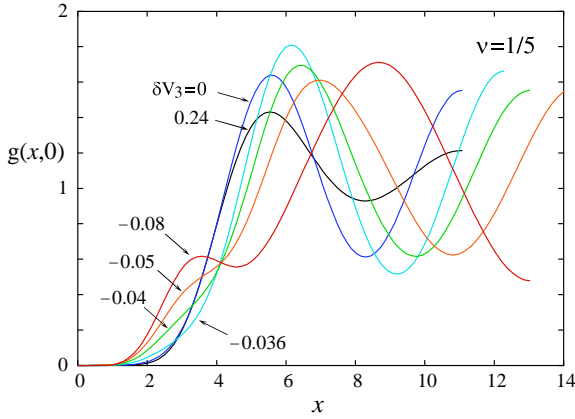


Fig. 8. Ground state pair correlation functions on the x -axis at $\nu = 1/5$ for various δV_3 . $N_e = 12$. $\delta V_3 = 0$ corresponds to pure Coulomb interaction.

of Wigner crystal at finite ν , we next see pair correlation functions in the ground state at low fillings. The ground state pair correlation functions below $\nu = 3/8$ in Figs. 5 and 9 (a) show that the stripe structure remains stable down to $\nu \sim 1/6$, although it seems to approach hexagonal structure of Wigner crystal.

At $\nu = 1/6$ the Wigner crystal is realized in an excited state close to the ground state. The correlation function of the Wigner crystal and the energy difference from the ground state are shown in Fig. 9 (b) and (c). The energy difference almost linearly decreases with decreasing ν except at $\nu = 1/5$, where the ground state is characterized by Laughlin state. Linear extrapolation on ν shows the crossing of the two energy levels at around $\nu = 1/7$. Since the momentum of the two states are different, we expect first order transition to the Wigner crystal at $\nu_c \sim 1/7$. The value of the critical filling ν_c is consistent with previous studies,^{28,29)} although exact diagonalizations of 6-electrons predict second order or weak first order transition.²⁹⁾

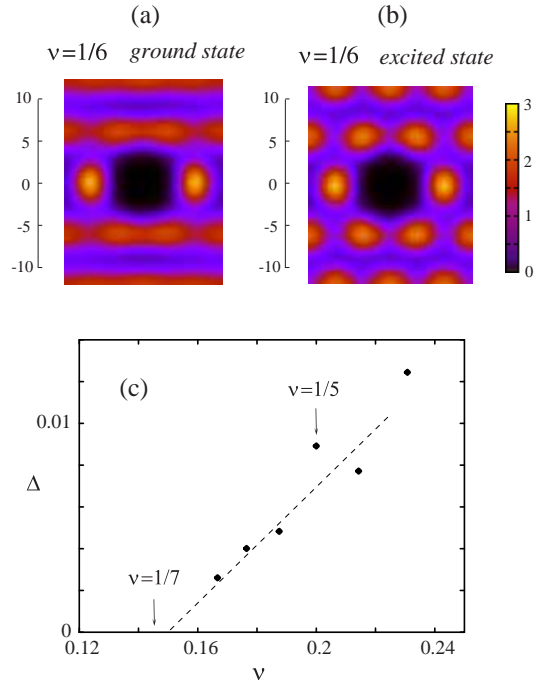


Fig. 9. (a) The ground state pair correlation function at $\nu = 1/6$. (b) The pair correlation function of Wigner crystal at $\nu = 1/6$. (c) Energy difference between the ground state and Wigner crystal at low fillings. $N_e = 12$. The dashed line is a guide for eyes.

3.6 Phase diagram of $N = 0$ Landau level

The present DMRG calculation shows the existence of four different ground states: the compressible liquid around $\nu = 1/2$, the incompressible liquid at $\nu = n/(2n+1)$ and $1/5$, the weak stripe state below $\nu \sim 0.42$, and Wigner crystal below $\nu_c \sim 1/7$. From the above results, the ground state phase diagram is determined as shown in Fig. 10. Precise critical fillings and the nature of the transitions are not clear for the boundary between the liquid states and the weak stripe state, but the transition to Wigner crystal is expected to be first order. The weak stripe structure found below $\nu \sim 0.42$ has clear oscillations along the stripes and this is clearly different from the stripe state realized in higher Landau levels. The ground state at $\nu = 1/5$ continuously connects to the Laughlin state realized in the limit of large V_1 and V_3 , while the size of the excitation gap is very small compared with the gap at $\nu = 1/3$. The pair correlation function at $\nu = 1/5$ is strongly modified from circularly symmetric one, because V_3 of the Coulomb interaction is located close to the boundary between Laughlin state and stripe state.

3.7 Pairing state at half filling in $N = 1$ Landau level

We next investigate the ground state in the second lowest Landau level. At $\nu_N = 1/2$, fractional quantum Hall

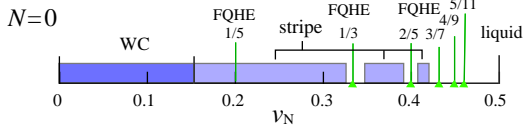


Fig. 10. Ground state phase diagram of the lowest Landau level determined by the DMRG method.

effect has been experimentally observed.¹⁴⁾ To explain the fractional quantization, p -wave pairing formation of electrons has been proposed.^{11,12,13)} In particular, recent studies based on exact diagonalizations suggest Pfaffian state of triplet spin pair.^{30,31)}

In the present study we introduce Haldane's pseudopotential V_1 in the second lowest Landau level. We calculate the excitation energies and the pair correlation functions at various V_1 . In Fig. 11 we show the total energy of the ground state and several low energy excited states as a function of δV_1 . We find two characteristic δV_1 where structure of the low energy spectrum changes. One is located slightly below $\delta V_1 = 0$ and the other is around $\delta V_1 = 0.03$ as shown in the figure by arrows. Below $\delta V_1 = 0$ the ground state is almost degenerate and the pair correlation function is characterized by clear stripes as shown in Fig. 12 (c). For $V_1 > 0.03$, the ground state and low energy excited states is almost independent of V_1 . The correlation function is circularly symmetric with weak oscillations as shown in Fig. 12 (a), and it is similar to that observed at $\nu = 1/2$ in the lowest Landau level, where excitation gap vanishes in the thermodynamic limit. Since sufficiently large δV_1 effectively maps the system onto the lowest Landau level, we expect that the ground state is compressible liquid for $\delta V_1 > 0.03$.

Between $\delta V_1 = 0.0$ and 0.03 , the ground state is clearly different from the stripe state. The correlation function clearly decays at long distance as shown in Fig. 12 (b) and the degeneracy in the ground state is lifted with a finite excitation gap of order 0.01 . Compared with the compressible liquid state at $\delta V_1 > 0.03$, the correlation function is different at short distance as shown in Fig. 12 (d), which shows the difference in the correlation function between $\delta V_1 = 0.01$ and 0.06 : $g(r)_{\delta V_1=0.01} - g(r)_{\delta V_1=0.06}$. In this figure, we can see that electrons are attracted around the origin $r \sim 1.5$ consistent with the pair formation.

3.8 Stripes away from half filling in $N = 1$ Landau level

We next investigate the ground state away from half filling. The pair correlation functions for $\nu = 4/9, 2/5, 4/11$, and $1/3$ with 16 electrons in the unit cell are presented in Fig. 13. These results clearly show the existence of the stripe correlations even in the second lowest Landau level near half filling. In order to see detailed structure of the stripes we show the correlation functions on the x and y axes in Fig. 14. As is shown, the correlation function on the y -axis at $\nu = 4/9$ and

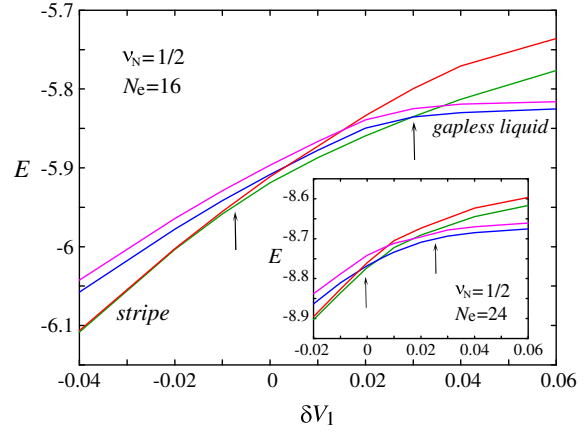


Fig. 11. Low energy spectrum at half filling in the second lowest Landau level. $N_e = 16$. Inset shows the results for $N_e = 24$. $\delta V_1 = 0$ corresponds to pure Coulomb interaction.

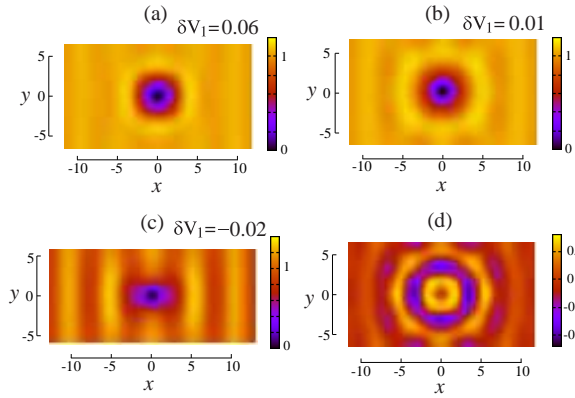


Fig. 12. The ground state pair correlation functions in guiding center coordinates at half filling in the second lowest Landau level at $\delta V_1 = 0.06$ (a), 0.01 (b), and -0.02 (c). Figure (d) shows the difference in the correlation function between $\delta V_1 = 0.01$ and $\delta V_1 = 0.06$, $g(r)_{\delta V_1=0.01} - g(r)_{\delta V_1=0.06}$. $N_e = 24$.

$2/5$ shows monotonic increase from the origin and it becomes almost constant at a long distance. This is the same structure of the stripes observed in higher Landau levels near half filling as shown in Fig. 15. Compared with the stripes in $N = 2$ Landau level, the amplitude of the oscillations on the x -axis is about 50% smaller and their period is 30% shorter. This means the strips in $N = 1$ Landau level is likely to be disturbed by residual potential fluctuations and temperatures. We think this may be a reason why anisotropic resistivity is not clearly observed in the second lowest Landau level.

With further decreasing ν , character of the stripes changes at $\nu \sim 4/11$. This is clearly shown in the correlation functions along the stripes in Fig. 14. The correlation function for $\nu < 4/11$ shows weak oscillations along the stripes, which is similar to the stripe structure in the lowest Landau level. The oscillations on the stripes are enhanced with decreasing ν and the ground state becomes almost the same to that in the lowest Landau level

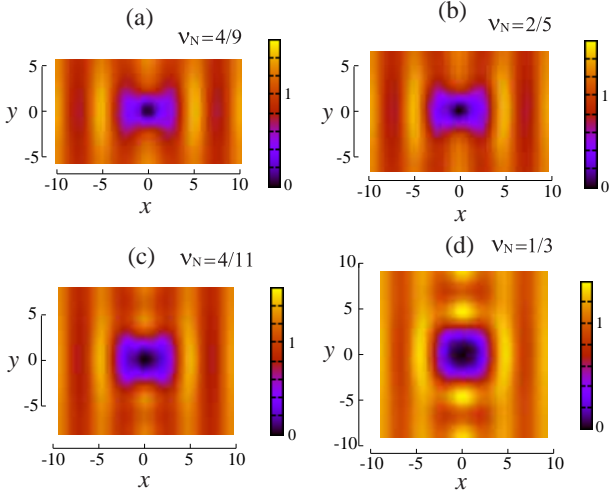


Fig. 13. The ground state pair correlation functions in guiding center coordinates in the second lowest Landau level near half filling. $N_e = 16$.

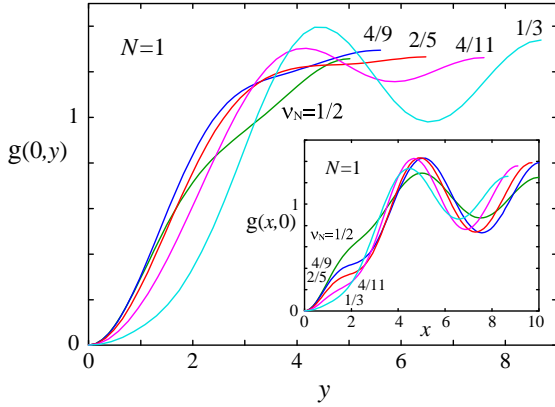


Fig. 14. The ground state pair correlation functions on the y -axis in guiding center coordinates in the second lowest Landau level. Inset shows the results on the x -axis. $N_e = 16$.

except at $\nu = 1/3$. At low fillings $\nu < 1/4$, the correlation functions in $N=0$ and 1 Landau levels are almost identical with each other. The similarity of the ground state between the two Landau levels at $\nu = 1/4$ has been shown by previous calculations.^{32,33)}

At $\nu = 1/3$, the ground state correlation function is clearly different from that of the lowest Landau level. Compared with Laughlin state in the lowest Landau level, short range correlation below $r \sim 2\ell$ is enhanced and clear oscillations exist at long distance as shown in Fig. 16. This is due to the large reduction of short range interaction V_1 , which stabilizes Laughlin state.

In order to see the effect of V_1 on the ground state, we show in Fig. 17 the energies of the ground state and excited state as a function of V_1 . The excitation gap

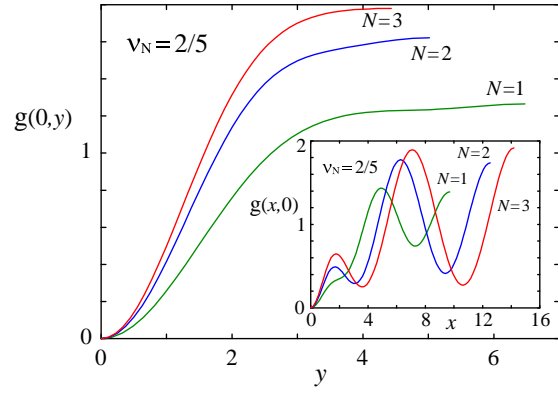


Fig. 15. The ground state pair correlation functions on the y -axis in guiding center coordinates in $N = 1, 2$, and 3 Landau levels at $\nu_N = 2/5$. Inset shows the results on the x -axis. $N_e = 16$.

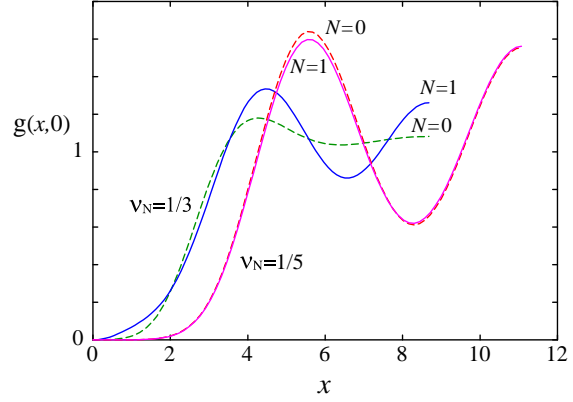


Fig. 16. The ground state pair correlation functions at $\nu_N = 1/3$ and $1/5$ in the lowest and the second lowest Landau levels.

monotonically increases with increasing V_1 from $\delta V_1 = 0$ and no phase transition is detected. Since the ground state at large V_1 is Laughlin state as shown in Fig. 18 (c), where the correlation functions at $\delta V_1 = 0.08$ is almost identical to that in the lowest Landau level, the present result shows the ground state at $\delta V_1 = 0$ continuously connects to Laughlin state. However, the excitation gap is very small at $\delta V_1 = 0$ compared with the gap in the lowest Landau level and slight decrease in V_1 leads to the transition to stripe state as shown in Fig. 17. The correlation function of the stripe state at $\delta V_1 = -0.02$ is shown in Fig. 18 (b), which is similar to the stripe state near half filling. With further decreasing V_1 , first order transition to two-electron bubble phase occurs at $\delta V_1 \sim -0.04$. This is consistent with the results in higher Landau levels, where bubble state is realized at $\nu_N = 1/3$ in $N = 2$ Landau level.^{17,34,35,36)}

In contrast to the ground state at $\nu_N = 1/3$, the correlation function at $\nu_N = 1/5$ is almost the same to that in the lowest Landau level as shown in Fig. 16. This is not surprising because V_3 of the second lowest Landau level is larger than that of the lowest Landau level.

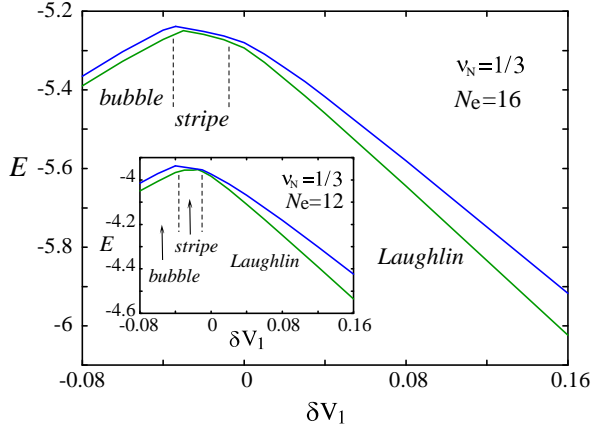


Fig. 17. The ground state and first excited state energies in the second lowest Landau level at $\nu_N = 1/3$ with $N_e = 16$. Inset shows the results for $N_e = 12$. $\delta V_1 = 0$ corresponds to pure Coulomb interaction.

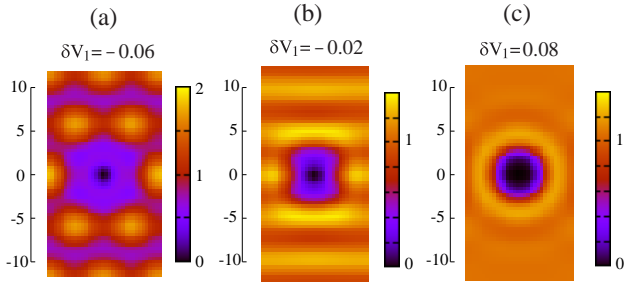


Fig. 18. The ground state pair correlation functions in guiding center coordinates in the second lowest Landau level at $\nu_N = 1/3$ with $N_e = 16$.

Since Laughlin state at $\nu_N = 1/5$ is stabilized by V_1 and V_3 , large V_3 compared with other V_m stabilizes Laughlin state similarly to the lowest Landau level, although circularly symmetric correlation function is strongly modified by the presence of other pseudo-potentials V_m of Coulomb interaction.

3.9 Transition to Wigner crystal

At sufficiently small ν_N , the Wigner crystal is realized in the ground state even in high Landau levels, because electrons can be treated as point particles when mean distance between the electrons becomes much longer than typical length scale of the one-particle wave function. In order to study the transition to Wigner crystal in the second lowest Landau level, we calculate the energy of Wigner crystal and compare with the ground state energy. The energy difference between the two states and

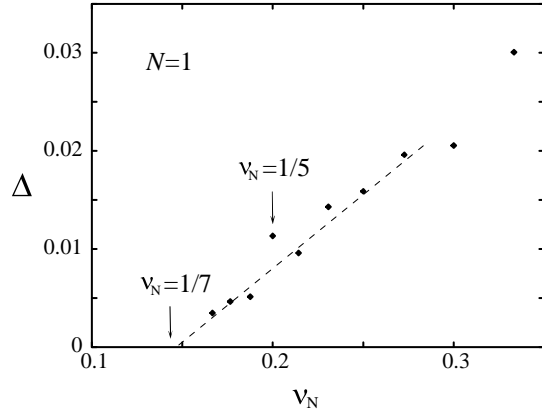


Fig. 19. Energy difference between Wigner crystal and the ground state. $N_e = 12$. The dashed line is a guide for eyes.

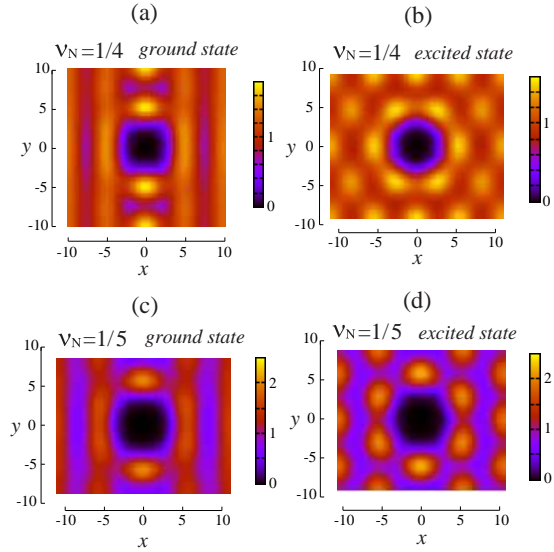


Fig. 20. Pair correlation functions in guiding center coordinates in the second lowest Landau level. (a) The ground state at $\nu_N = 1/4$ with 16 electrons. (b) Wigner crystal at $\nu_N = 1/4$ with 16 electrons obtained at a different total momentum from the ground state. (c) The ground state at $\nu_N = 1/5$ with 12 electrons. (d) Wigner crystal at $\nu_N = 1/5$ with 12 electrons.

the correlation functions of the guiding center are shown in Figs. 19 and 20, respectively. The energy difference between the two states monotonically decreases except at $\nu_N = 1/5$, where the ground state continuously connects to Laughlin state. The singular behavior at $\nu_N = 1/5$ is due to the decrease in the ground state energy. The linear extrapolation of the energy difference with respect to ν_N shows first order transition to Wigner crystal at $\nu_N \sim 1/7$.

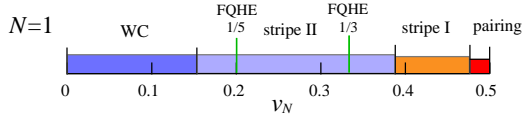


Fig. 21. Ground state phase diagram of the second lowest Landau level determined by the DMRG method.

3.10 Phase diagram of $N = 1$ Landau level

The ground state phase diagram of the second lowest Landau level is shown in Fig. 21. At half filling, the ground state pair correlation function suggests pairing state. This ground state is different from both the stripe state in higher Landau levels and the compressible liquid state in the lowest Landau level. With decreasing ν_N , however, stripe state similar to that in higher Landau levels is realized with small amplitude of the stripes (stripe I), which is 50% smaller than that in $N = 2$ Landau level. With further decreasing ν_N , clear oscillations along the stripes appear below $\nu \sim 4/11$ (stripe II). This structure is similar to the stripes in the lowest Landau level. At $\nu_N = 1/3$, the ground state belongs to the same phase of Laughlin state in the lowest Landau level, but correlation function shows clear oscillations at long distance. This is due to the proximity to the boundary between Laughlin state and stripe state. Below $\nu_N \sim 1/4$, the correlation functions are almost identical to that in the lowest Landau level, and thus the ground state is almost the same between the two Landau levels. The ground state at $\nu_N = 1/5$ is expected to be in the same phase of Laughlin state. The first order transition to Wigner crystal is expected to occur at $\nu_N \sim 1/7$.

§4. Summary and Discussion

In the present paper we have studied ground state pair correlation functions and low energy excitations of 2D electrons in the lowest and the second lowest Landau levels by using DMRG method. We have assumed completely spin polarized state and neglected Landau level mixing. The obtained results in the lowest Landau level confirmed the existence of compressible liquid at $\nu = 1/2$, incompressible liquid at $\nu = n/(1 + 2n)$ and $1/5$, and Wigner crystal below $\nu \sim 1/7$. We have found new stripe state between $\nu \sim 0.42$ and $1/7$, whose correlation function shows oscillations along the stripes, which is different from the stripes in higher Landau levels. In the second lowest Landau level, pairing state at $\nu_N = 1/2$ has been confirmed. The ground state is close to the phase boundary between the pairing state and stripe state, and decrease in V_1 of about 2% is enough for the transition to the stripe state. Between $\nu_N \sim 0.47$ and 0.38 we have found stripe state similar to that in higher Landau levels with small amplitude of stripes. We have also found stripe state similar to that in the lowest Landau level between $\nu_N \sim 0.38$ and $1/7$. At low fillings $\nu_N < 1/3$, the ground state is almost the same to that in the lowest Landau level. This is due to the fact that V_2

of the second lowest Landau level, which is the dominant interaction for $\nu_N < 1/3$, is slightly increased from that in the lowest Landau level, and this increase stabilizes the ground state realized in the lowest Landau level.

We have also shown the existence of incompressible liquids at $\nu_N = 1/3$ and $1/5$ in the second lowest Landau level. The size of the gap at $\nu_N = 1/3$ is very small compared with that in the lowest Landau level and slight decrease in V_1 of about 0.01 leads to the transition to stripe state. In actual systems, the wave function has finite width in the direction perpendicular to the two-dimensional plane. Since finite width reduces V_1 from the value of ideal two dimensional system, incompressible liquid at $\nu_N = 1/3$ will not be realized in systems of wide quantum well. Our estimate shows the critical width is about 4ℓ for rigid density distribution in the direction perpendicular to the two-dimensional plane in square potential well.

Recent experiment on the second lowest Landau level shows that there exist reentrant integer quantum Hall states around $\nu_N = 0.42$ and $\nu_N = 0.25$.¹⁵⁾ Our results suggest reentrant phase around $\nu_N = 0.42$ corresponds to the stripe phase near half filling, although the mechanism of the integer quantum Hall effect is still not clear. Since the amplitude of the stripes is small compared with that of higher Landau levels, it is expected that weak random potentials disturb stripe correlations and insulating state pinned by residual potential fluctuations is realized before forming stripe state.

Concerning to the reentrant phase around $\nu_N = 0.25$, similar behavior is expected in the lowest Landau level, since the ground state obtained in the present calculation is almost the same between the two Landau levels. This means the origin of insulating behavior above $\nu = 1/5$ in the lowest Landau level is the same to that of the reentrant phase around $\nu_N = 0.25$ in the second lowest Landau level. Since the energy of Wigner crystal is close to the ground state energy, it may be possible that random potentials stabilize pinned Wigner crystal, which is the same mechanism of integer quantum Hall effect at small $\nu_N < 1/7$.

Acknowledgement

The present work is supported by Grant-in-Aid No. 14540294 and No. 11740184 from JSPS.

-
- [1] R.B. Laughlin: Phys. Rev. Lett. **50** (1983) 1395.
 - [2] D.C. Tsui, H.L. Störmer and A.C. Gossard: Phys. Rev. Lett. **48** (1982) 1599.
 - [3] D. Yoshioka: Phys. Rev. B **29** (1984) 6833.
 - [4] H.W. Jiang, H.L. Stormer, D.C. Tsui, L.N. Pfeiffer and K.W. West: Phys. Rev. B **44** (1991) 8107; H. W. Jiang, R.L. Willett, H.L. Stormer, D.C. Tsui, L.N. Pfeiffer and K.W. West: Phys. Rev. Lett. **65** (1990) 633.
 - [5] P.D. Ye, L.W. Engel, D.C. Tsui, R.M. Lewis, L.N. Pfeiffer, and K. West: Phys. Rev. Lett. **89** (2002) 176802.
 - [6] A.A. Koulakov, M.M. Fogler, and B.I. Shklovskii: Phys. Rev. Lett. **76** (1996) 499.
 - [7] M.M. Fogler, A.A. Koulakov, and B.I. Shklovskii: Phys. Rev. B **54** (1996) 1853.
 - [8] M.P. Lilly, K.B. Cooper, J.P. Eisenstein, L. N. Pfeiffer, and K. W. West: Phys. Rev. Lett. **82** (1999) 394.

- [9] R.R. Du, D.C. Tsui, H.L. Stormer, L.N. Pfeiffer, K. W. Baldwin, and K. W. West: Solid State Commun. **109** (1999) 389.
- [10] K.B. Cooper, M.P. Lilly, J.P. Eisenstein, L. N. Pfeiffer, and K. W. West: Phys. Rev. B **60** (1999) R11285.
- [11] F.D.M. Haldane and E.H. Rezayi: Phys. Rev. Lett. **60** (1988) 956.
- [12] M. Greiter, X.G. Wen, and F. Wilczek: Phys. Rev. Lett. **66** (1991) 3205.
- [13] G. Moore and N. Read: Nucl. Phys. B **360** (1991) 362.
- [14] W. Pan, J.-S. Xia, V. Shvarts, D.E. Adams, H.L. Stormer, D.C. Tsui, L.N. Pfeiffer, K.W. Baldwin, and K.W. West: Phys. Rev. Lett. **83** (1999) 3530.
- [15] J. P. Eisenstein, K. B. Cooper, L. N. Pfeiffer, and K. W. West: Phys. Rev. Lett. **88** (2002) 076801.
- [16] S.R. White: Phys. Rev. Lett. **69** (1992) 2863; Phys. Rev. B **48** (1993) 10345.
- [17] N. Shibata and D. Yoshioka: Phys. Rev. Lett. **86** (2001) 5755.
- [18] J.K. Jain: Phys. Rev. Lett. **63** (1989) 199; Phys. Rev. B **40** (1989) 8079.
- [19] B.I. Halperin, P.A. Lee, and N. Read: Phys. Rev. B **47** (1993) 7312.
- [20] R.R. Du, H.L. Stormer, D.C. Tsui, A.S. Yeh, L.N. Pfeiffer, and K.W. West: Phys. Rev. Lett. **73** (1994) 3274.
- [21] M. Onoda, T. Mizusaki, T. Otsuka, and H. Aoki: Phys. Rev. Lett. **84** (2000) 3942.
- [22] R.R. Du, H.L. Stormer, D.C. Tsui, L.N. Pfeiffer, and K.W. West: Phys. Rev. Lett. **70** (1993) 2944.
- [23] W. Pan, H.L. Stormer, D.C. Tsui, L.N. Pfeiffer, K.W. Baldwin, and K.W. West: Phys. Rev. Lett. **88** (2002) 176802.
- [24] S.S. Mandal and J.K. Jain: Phys. Rev. B **66** (2002) 155302.
- [25] S.-Y. Lee, V.W. Scarola, and J.K. Jain: Phys. Rev. Lett. **87** (2001) 256803.
- [26] S.-Y. Lee, V.W. Scarola, and J.K. Jain: Phys. Rev. B **66** (2002) 085336.
- [27] F.D.M. Haldane and E.H. Rezayi: Phys. Rev. Lett. **54** (1985) 273.
- [28] P.K. Lam and S.M. Girvin: Phys. Rev. B **30** (1984) 473.
- [29] Kun Yang, F.D.M. Haldane, and E.H. Rezayi: Phys. Rev. B **64** (2001) 081301.
- [30] R. H. Morf: Phys. Rev. Lett. **80** (1998) 1505.
- [31] E.H. Rezayi and F.D.M. Haldane: Phys. Rev. Lett. **84** (2000) 4685.
- [32] R. Morf and N. d'Ambrumenil: Phys. Rev. Lett. **74** (1995) 5116.
- [33] M. Onoda, T. Mizusaki, and H. Aoki: preprint.
- [34] M.M. Fogler and A.A. Koulakov: Phys. Rev. B **55** (1997) 9326.
- [35] F.D.M. Haldane, E.H. Rezayi, and Kun Yang: Phys. Rev. Lett. **85** (2000) 5396.
- [36] D. Yoshioka and N. Shibata: Physica E **12** (2002) 43.